Characterization of Murine Astrocyte Cultures in 3D Hydrogel Matrices

An Approach to Nuclei Segmentation and Assisted Cell Classification

Maria Beatriz Sereno Fernandes

Thesis to obtain the Master of Science Degree in

Biomedical Engineering

Supervisors: Dr. Thomas Distler
Dr. Giacomo Masserdotti
Prof. Rui Henriques

Examination Committee: Prof. João Miguel Raposo Sanches
Prof. Rui Miguel Carrasqueiro Henriques
Prof. Daniel Pedro de Jesus Faria

March 2025

Contents

Motivation

Astrocytes in Neuroscience Research

➢ Most abundant glial cell type in the mammalian CNS

➢ Very heterogeneous cell population (Bocchi et al., 2025)

➢ Potential for therapeutic applications via direct neural reprogramming (Pereira et al., 2024)
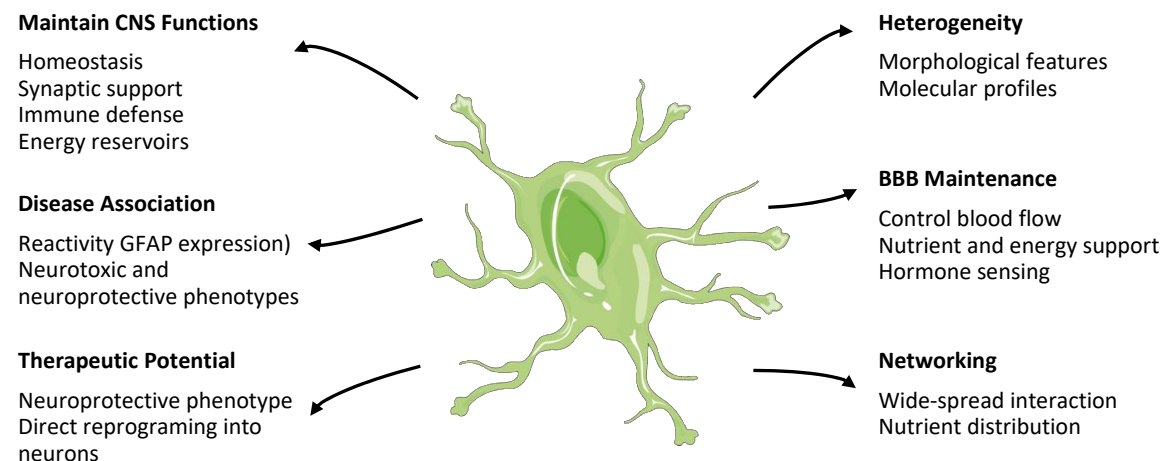
Maintain CNS Functions

Homeostasis
Synaptic support
Immune defense
Energy reservoirs

Disease Association

Reactivity GFAP expression)
Neurotoxic and
neuroprotective phenotypes

Therapeutic Potential

Neuroprotective phenotype
Direct reprograming into
neurons

Heterogeneity

Morphological features
Molecular profiles

BBB Maintenance

Control blood flow
Nutrient and energy support
Hormone sensing

Networking

Wide-spread interaction
Nutrient distribution

Protoplasmic

Fibrous

Figure 1.1. Astrocytes main characteristics. Adapted from Garland et al. (2022).
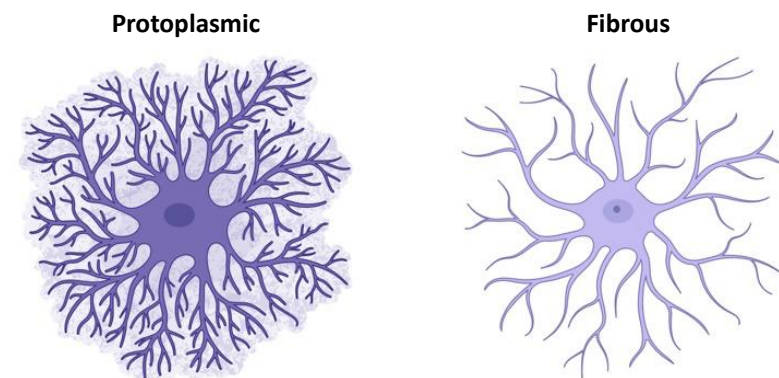
Figure 1.2. Astrocytes morphological heterogeneity. Created in BioRender.

Bocchi et al. (2025). Astrocyte heterogeneity reveals region-specific astrogenesis in the white matter. https://doi.org/10.1038/s41593-025-01878-6
Garland et al. (2022). Microglia and astrocyte function and communication: what do we know in humans?. https://doi.org/10.3389/fnins.2022.824888
Pereira et al. (2024). Direct neuronal reprogramming of mouse astrocytes is associated with multiscale epigenome remodeling and requires Yy1. https://doi.org/10.1038/s41593-024-01677-5

Motivation

Optimize Hydrogel Models

➢ Limitations of current 2D models to mimic brain structure and physicochemical properties

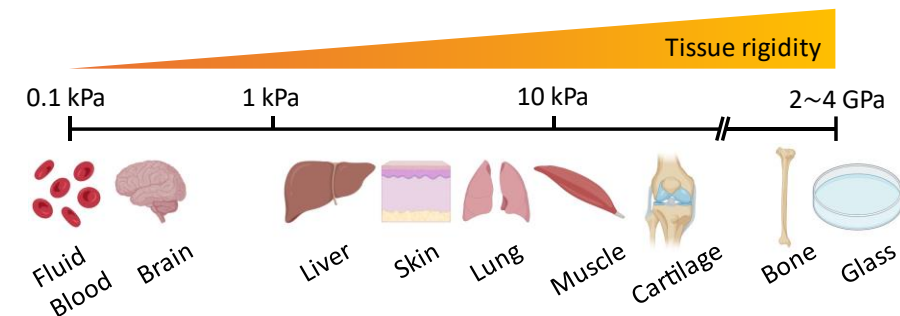➢ Potential of resembling brain physicochemical properties and microenvironment

Figure 1.3. Rigidity scale of different tissues and glass (adapted from Park et al. 2022).
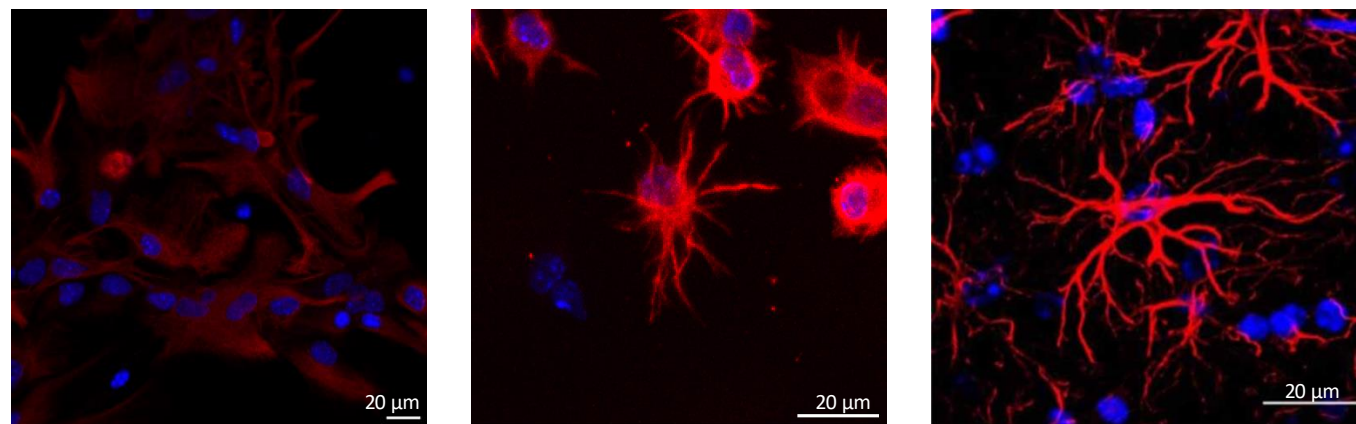

A. Monolayer PDL   **B.** Hydrogel substrate   **C.** Murine brain

Figure 1.4. Astrocytes morphology grown in different environments. **(A)** and **(B)** 7 DIV cultures (from this Master's thesis), and **(C)** Ex vivo morphology from Matias et al. (2019).

Park et al. (2022). Materials and extracellular matrix rigidity highlighted in tissue damages and diseases: Implication for biomaterials design and therapeutic targets. https://doi.org/10.1016/j.bioactmat.2022.06.003
Matias et al. (2019). Astrocyte Heterogeneity: Impact to Brain Aging and Disease. https://doi.org/10.3389/fnagi.2019.00059

Motivation

Automate Biological Image Analysis

Challenges:

- ➢ Biological image annotation is very time consuming

- ➢ 3D stack annotation is challenging

Opportunities:

- ➢ Potential to automate annotation process

- ➢ Advances in computer vision technologies allow accurate identification of objects

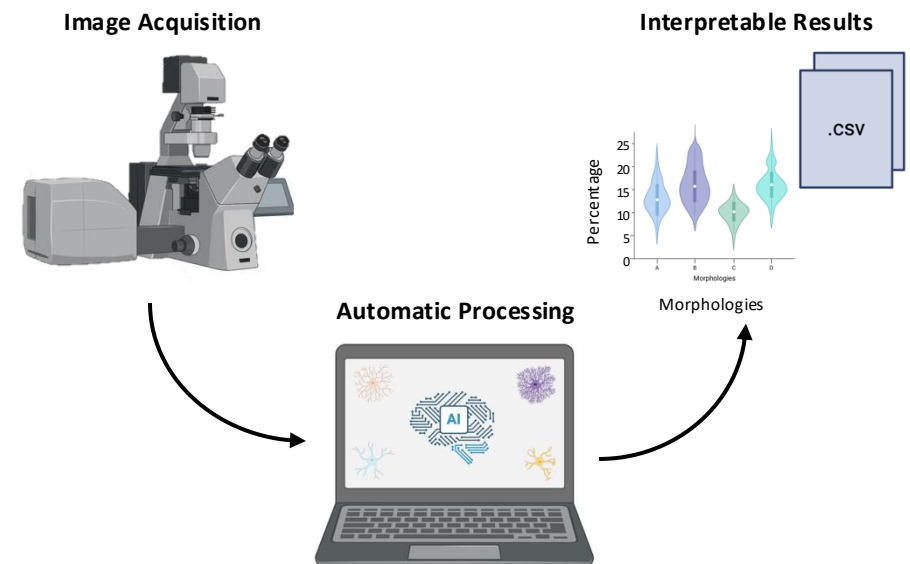- ➢ High-throughput characterization of cultures

Image Acquisition

Interpretable Results

Automatic Processing

Figure 1.5. Pipeline overview for automatic image analysis.

Research Objectives

Computational Work

➢ Train nuclei segmentation models for hydrogel cultures

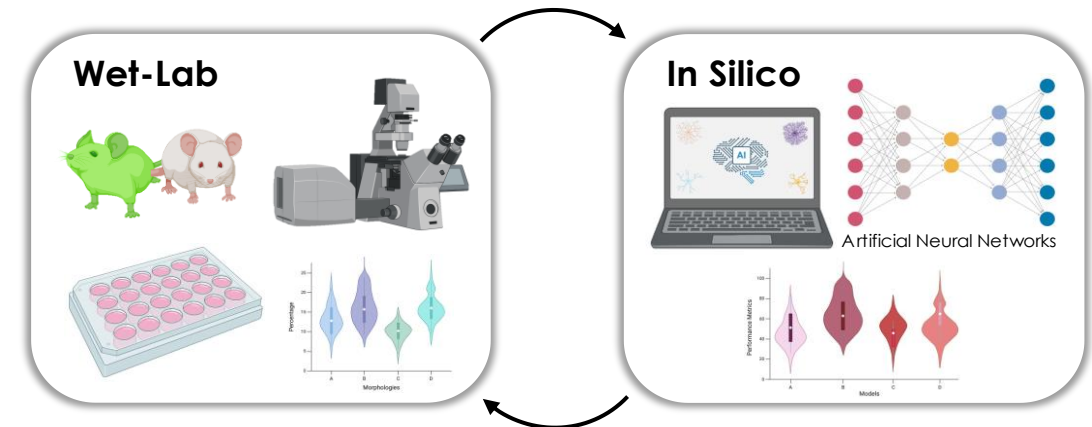➢ Co-develop GUI for z-stack image annotation

Figure 1.6. Ilustrative scheme of project tasks.

Experimental Work

➢ Prepare murine gray matter-derived astrocyte cultures in hydrogels

➢ Compare astrocyte 3D **morphology** in different hydrogel substrates (MVG, VLVG, Fibrin, FibrinVLVG)

➢ Analyse of **expression astrocyte markers** in different hydrogels and PDL cultures (SOX9, GFAP)

➢ Study the **effect of CaCl$_2$ concentration** used for hydrogel gelling on cell viability, morphology and astrocyte marker expression

02 Computational Work

Machine Learning for Biomedical Data Analysis

Biomedical Data Analysis

- Drug discovery
- Precision healthcare
- Protein structure prediction
- Omics/Multi-omics
- Risk prediction prognosis
- Clinical decision support
- Therapeutic assistance
- Medical and **biological image analysis**

Biological Imaging

- Observe biological processes and the cellular and molecular levels
- High volumes of data
- Absence of standardized protocols
- High variability of experimental conditions

Need of Automation
- High-throughput data analysis
- Enhance reproducibility of data analysis

Vs.

Hurdles of Automation
- Heterogeneity of datasets
- High data variability

Deep Learning for Biological Image Analysis

| Classification | Object Detection | Instance Segmentation | Semantic Segmentation |

Highly branched cell | Round cell, Branched cell, Highly branched cell | nuclei 1, nuclei 2, ..., nuclei N | Background, Nuclei border, Nuclei body
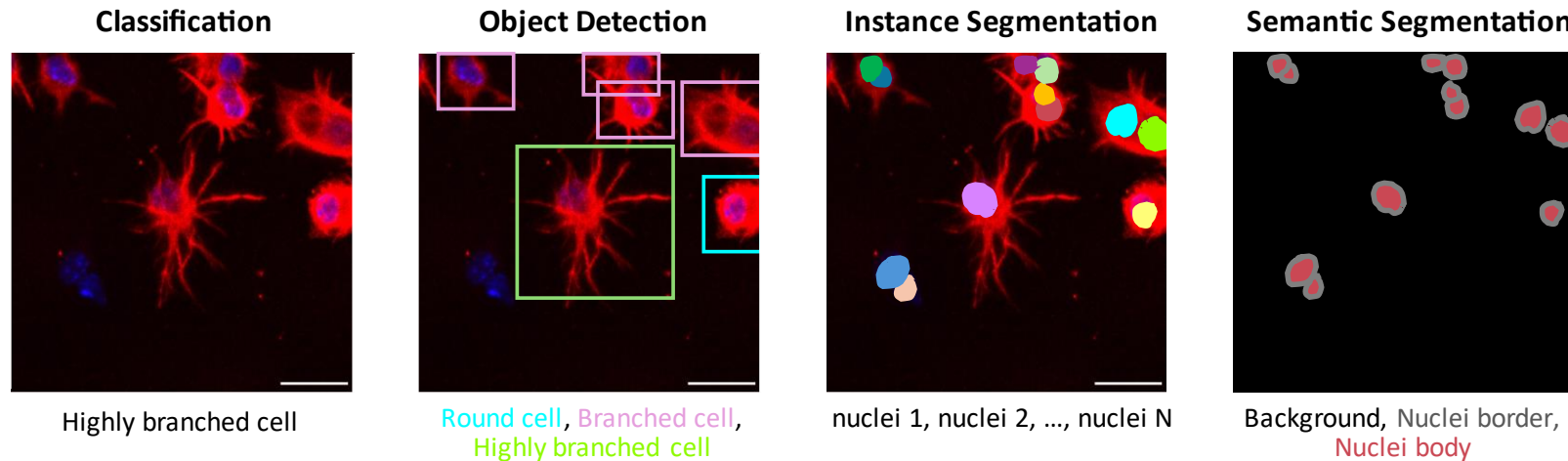
Figure 2.3. Outlook of computer vision tasks in the context of astrocyte culture characterization.

Convolutional Neural Networks (CNNs)

➢ Sparse interactions

➢ Parameter sharing

➢ Equivariance to translation

Open-source Architectures for Segmentation

➢ U-Net, nnU-Net

➢ Mask R-CNN

➢ Stardist 2D, Stardist 3D

➢ Cellpose and Cellstitch

3D Nuclei Segmentation
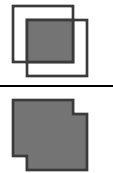
Training and Testing Dataset

➤ 16 z-stack images

➤ Murine-derived astrocyte cultures in 3D hydrogel matrices

➤ 200.63 x 200.63 x 200 μm³

➤ DAPI and GFAP channel

Architectures

➤ nnU-Net

➤ Stardist 3D

➤ Cellstitch

Evaluation Metrics

➤ $IoU = \dfrac{Area\ of\ overlap}{Area\ of\ union} = \dfrac{A \cap B}{A \cup B}$

➤ $precision_\tau = \dfrac{TP}{TP+FP}$

➤ $recall_\tau = \dfrac{TP}{TP+FN}$

➤ $mAP_\tau = \dfrac{TP}{TP+FP+FN}$

➤ $F1\ score_\tau = \dfrac{2*precision*recall}{precision+recall}$

➤ $PR = \dfrac{\#\ predictions}{\#\ GT\ predictions} = \dfrac{TP+FP}{TP+FP+FN}$

➤ $AR = \dfrac{\#\ aggregated\ predictions}{TP+FP+FN}$

Results: 3D Nuclei Segmentation

nnU-Net Outperforms Stardist 3D and Cellstitch

➢ nnU-Net closer to optimal values in all assessed metrics

➢ Stardist 3D **underestimates** the number of nuclei

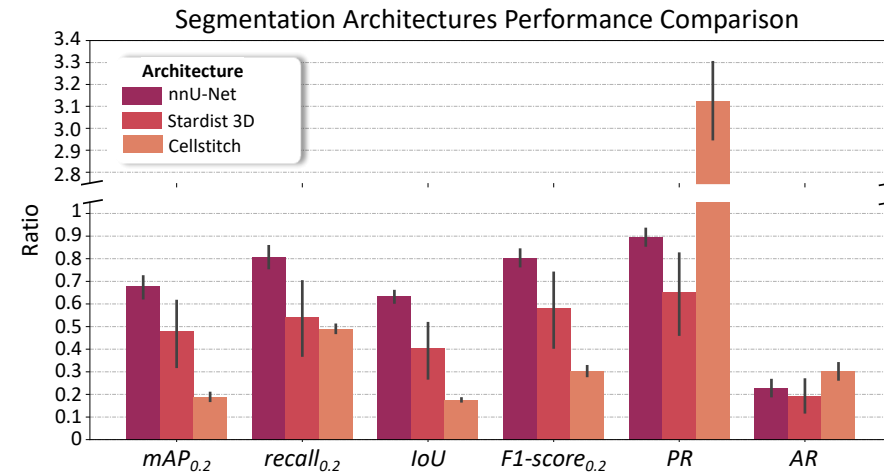➢ Cellstitch **overestimates** the number of nuclei

Figure 2.5. Performance of nnU-Net, Stardist 3D and Cellstitch. Error bar: 95% confidence interval.

Results: 3D Nuclei Segmentation

Improving nnU-Net Performance

➤ Transform the training dataset

➤ FOV range relates to nuclei relative size in the images

Table 2.3. Depiction of datasets generated for nnU-Net model enhancement.

Features	dataset 1	dataset 2	dataset 3	dataset 4	dataset 5
Images	preprocessed	raw	raw	raw + augmented	raw + augmented
Size	16	16	16	120	150
Selected Channels	DAPI + GFAP	DAPI + GFAP	DAPI	DAPI	DAPI
Augmentation	–	–	–	rotations, vertical and horizontal flips	rotations, vertical and horizontal flips, zoom
Digital Size (512,512,101,Z)	Z = 2	Z = 2	Z = 1	Z = 1	Z = 1
Training FOV Range (μm^2)	200.63	200.63	200.63	200.63	100.31 – 802.50
nnU-Net model	model 1	model 2	model 3	model 4	model 5

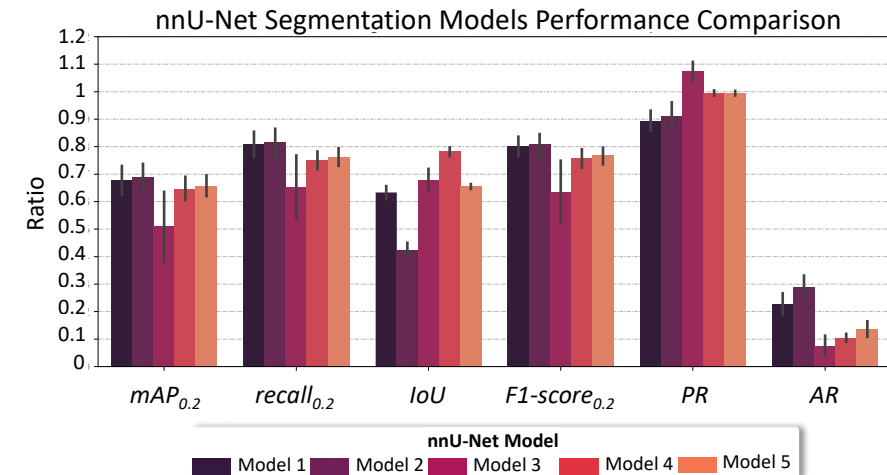## Enhanced nnU-Net Models Achieve Outstanding Prediction Ratios

Figure 2.6. Performance of nnU-Net enhanced models. Error bar: 95% confidence interval.

Table 2.4. Scoring of trained nnU-Net models.

Model	recall$_{0.2}$	precision$_{0.2}$	mAP$_{0.2}$	IoU	PR	AR	Score
model 1	2	2	2	4	5	4	20
model 2	1	1	1	5	4	5	17
model 3	5	5	5	2	3	1	21
model 4	4	4	4	1	2	2	17
model 5	3	3	3	3	1	3	16

Results: 3D Nuclei Segmentation

nnU-Net model successfully generalizes to unseen hydrogel cultures datasets
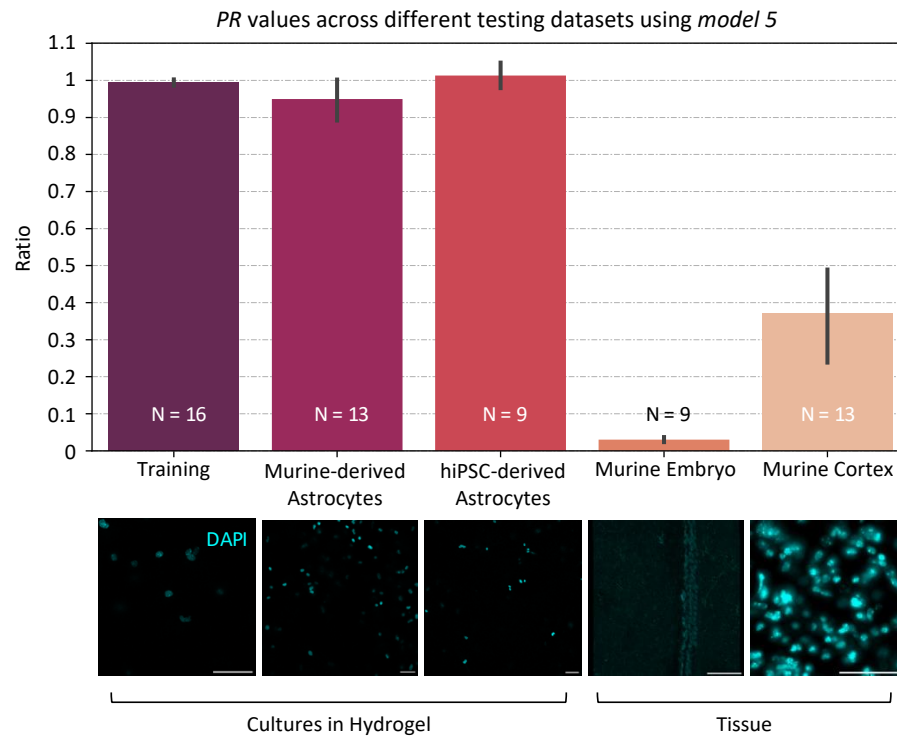
$$PR = \frac{\#\ predictions}{\#\ GT\ predictions} = \frac{TP + FP}{TP + FP + FN}$$

Figure 2.8. nnU-Net model 5 performance. **(A)** PR across the different testing datasets using model 5 as predictor. Error bar: 95% confidence interval. **(B)** Maximum intensity projections of images of each dataset. Scale bar = 50 μm. Z-stack depth = 12 μm.

GUI for Annotation of Z-stack Images

Image Visualization:

➢ Z-stack images: multilayer and multichannel

➢ Automatically adjusts channels to image loaded

Automatic Detection of Cells:

➢ Nuclei segmentation model to draw boxes around cell nuclei

➢ Additional facility to manually add missed instances

➢ Visualization of individual cell instances

Cell Classification:

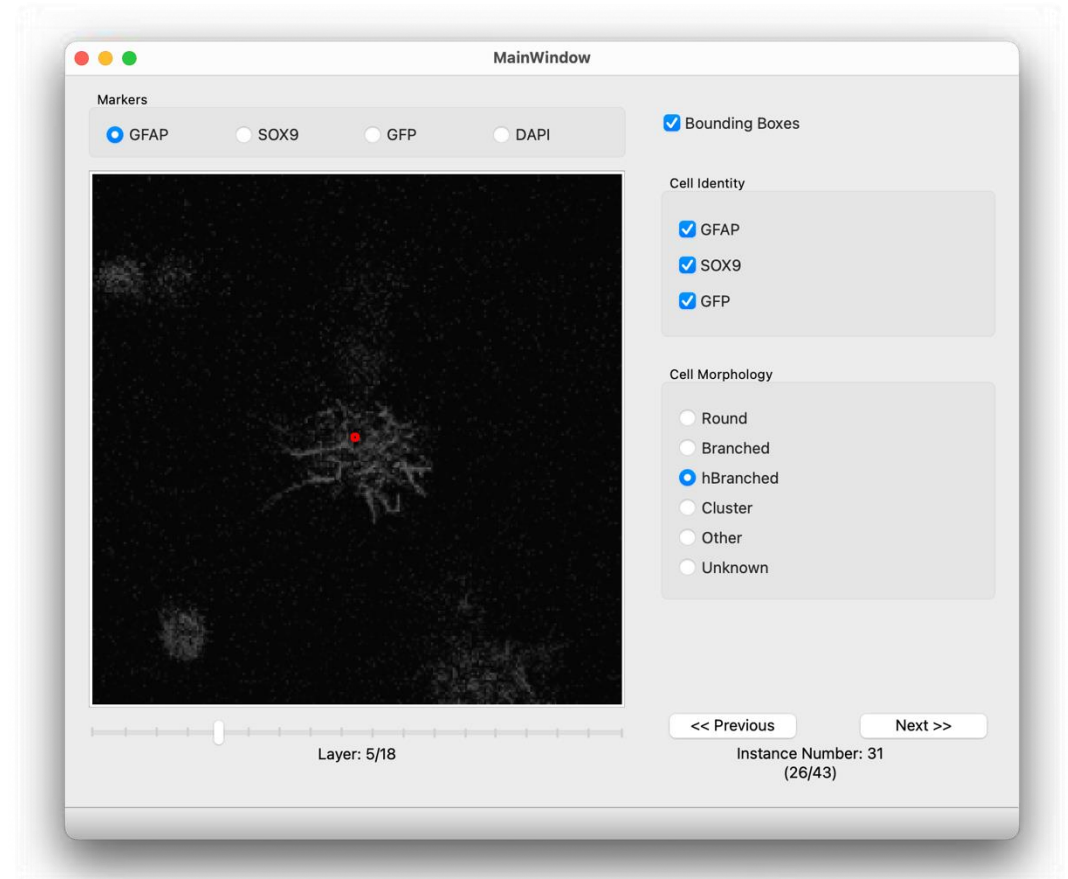➢ Semi-automatic prediction of markers expression

➢ Classification of cell morphology

Figure 2.11. GUI cell annotation window.

13

03 Experimental Work

Hydrogels

Alginate Hydrogels – MVG and VLVG

➢ Derived from brown algae – sodium alginate

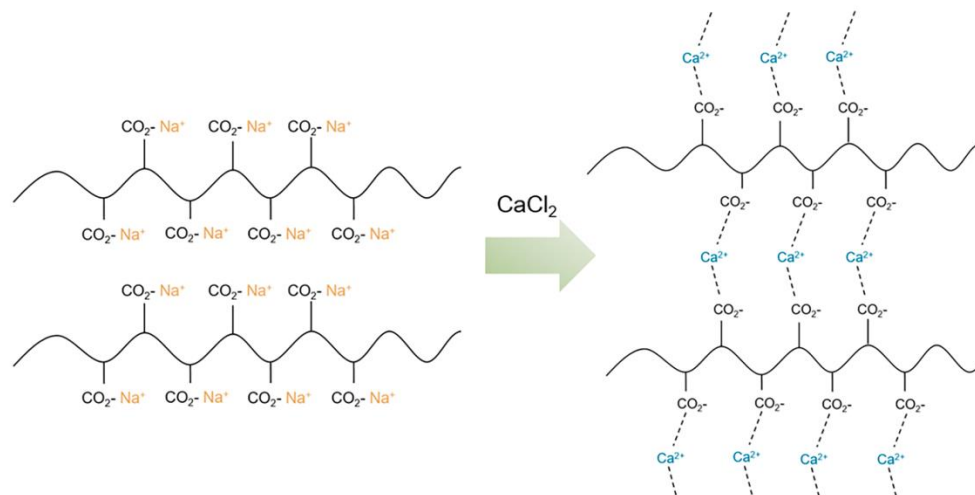➢ Polysaccharide-based hydrogel

➢ RGD motifs for cell adhesion

Fibrin Hydrogels

➢ Can be found in the ECM

➢ Fibrinogen is upregulated in response to lesion

➢ Might mimic closer brain injury than healthy conditions – fibrin is involved in coagulation cascade

Figure 3.1. Sodium alginate crosslinking.

Table 3.1. Summary of the hydrogels and crosslinking method used.

Abbreviation	Material	Crosslinking
MVG	Sodium alginate	100mM $CaCl_2$
VLVG	Sodium alginate	175mM $CaCl_2$
Fibrin	Fibrin + Thrombin	–
FibrinVLVG	Composite (VLVG alginate + fibrin, 1:1)	5, 50, 100, 175mM $CaCl_2$*

* Concentration dependent on experiment

MVG = Medium viscosity guluronate (222.000 g/mol; guluronic acid (GA) > 60%; 0.4% DOS RGD peptide)
VLVG = Very low viscosity guluronate (32.000 g/mol, GA > 60%, 0.376% DOS RGD peptide)

Astrocyte Markers

GFAP

➢ Glial Fibrillary Acidic Protein

➢ Cytoskeletal astrocyte marker

➢ Upregulated in reactive astrocytes and pathological conditions (Miller, 2018)

➢ Particularly prominent in fibrous astrocytes (Jurga, 2021)

SOX9

➢ SRY (sex determining region Y)-box transcription factor 9

➢ Nuclear transcription factor

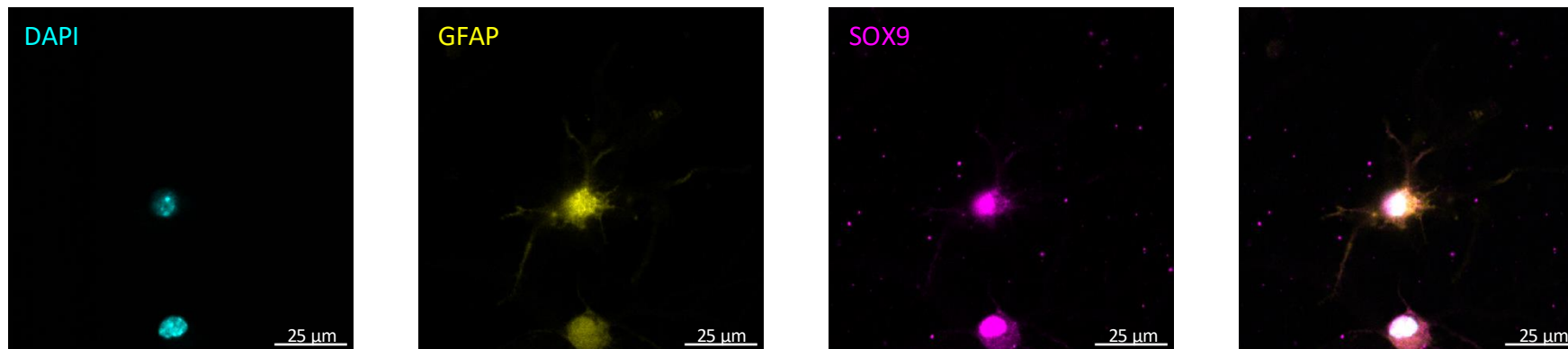➢ Pan-astrocyte marker, generally markers astrocytes in the CNS (Jurga, 2021) – labels almost all astrocytes

Figure 3.2. Astrocyte markers.

Miller (2018). Astrocyte heterogeneity in the adult central nervous system. https://doi.org/10.3389/fncel.2018.00401
Jurga et al. (2021). Beyond the GFAP-astrocyte protein markers in the brain. https://doi.org/10.3390/biom11091361

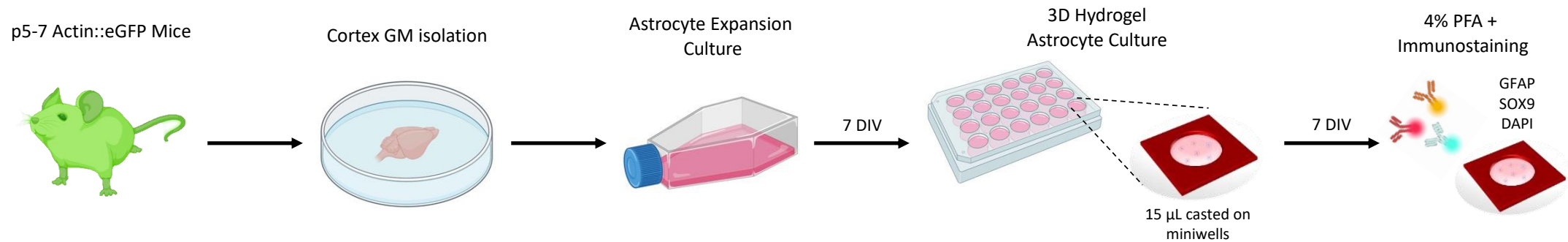# Validation of Alginate and Fibrin-Alginate Hydrogels

Figure 3.3. Procedure for the study of morphology and astrocyte marker expression in alginate and fibrin-alginate hydrogels.

Experimental conditions:

➢ 0.5% MVG – 100 mM CaCl$_2$

➢ 0.5% VLVG – 175 mM CaCl$_2$

➢ Fibrin + 0.5% VLVG (FibrinVLVG) – 175 mM CaCl$_2$

10^6 cells/mL

➢ PDL (2D control)

→ 0.25×10^6 cells/mL

Experiment:

➢ 3 biological replicates

➢ 2-4 technical replicates each

Morphology Categorization
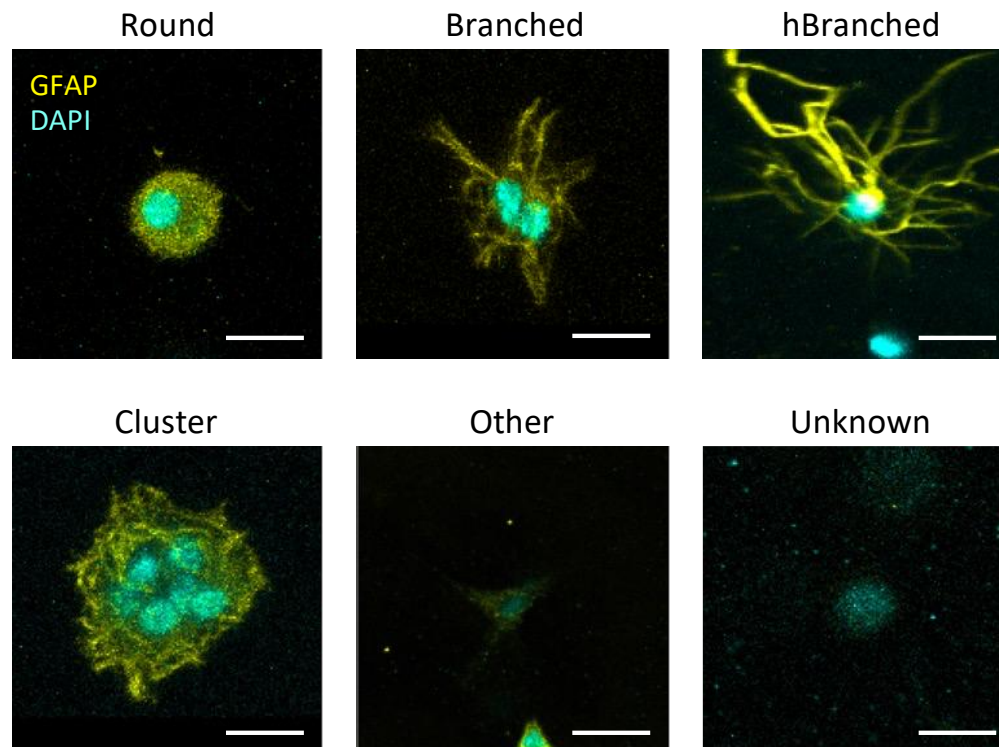
Figure 3.4. Representative cells of each morphology class.

Round cells: No branching

Branched cells: Some branching – cells with small branches and/or only 1 or 2 large branches, or branches that expand concentrically rather than radially

hBranched cells: Highly branched – cells with at least 3 large branches expanding radially

Clusters: cell agglomerates with at least 3 nuclei and no specific morphology

Other: Cells which morphology does not fit in any of the descriptions above

Unknown: Cells that are not stained with any cytoplasmic marker – impossible to categorize morphology

Result: FibrinVLVG hydrogels support **in vivo-like morphologies** and **increased GFAP⁺ reactive astrocytes**
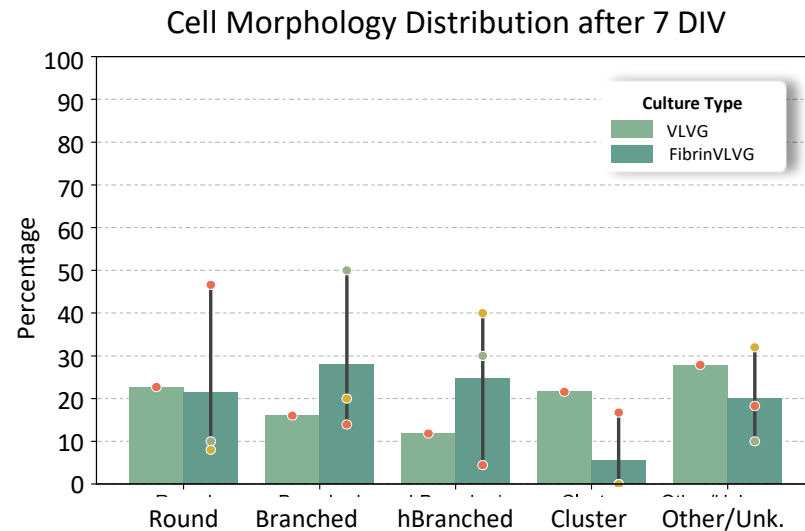

Cell Morphology Distribution after 7 DIV

Figure 3.5. Distribution of cell morphology in VLVG and FibrinVLVG after 7 DIV.

Markers Expression among DAPI⁺GFP⁺ cells after 7 DIV

Figure 3.6. Distribution of astrocyte marker expression in VLVG and FibrinVLVG after 7 DIV.

➢ FibrinVLVG have **less clusters** than VLVG hydrogels
(22% versus 6%)

➢ FibrinVLVG have **more branched cells**
(53% versus 38%)

➢ Astrocyte proportions, **SOX9⁺ (%) exceed 70%**

➢ Hydrogels show **higher GFAP⁺/SOX9⁺ reactive profiles**
(*t*-test, p = 0.15)

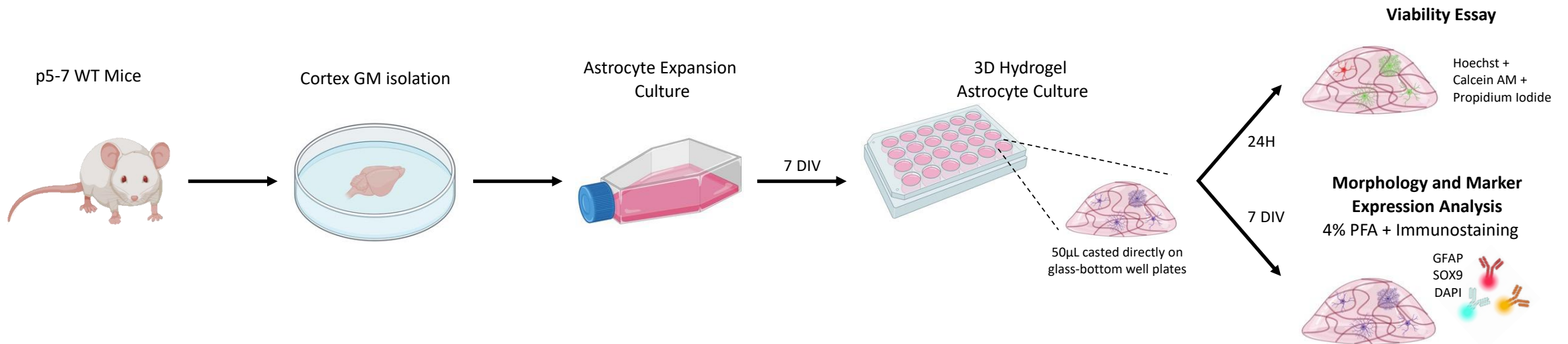# Effects of Different CaCl$_2$ Crosslinking Concentrations

Figure 3.7. Procedure to study the effects of CaCl$_2$ concentrations used for hydrogel crosslinking.

Experimental conditions:

➢ FibrinVLVG crosslinked with 5mM, 50mM, 100mM and 175mM CaCl$_2$

➢ Fibrin (0mM CaCl$_2$)

➢ PDL

10^6 cells/mL

0.25 x 10^6 cells/mL

Independent experiments:

1. Viability essay:
   ➢ 3 biological replicates
   ➢ 2-4 technical replicates each

2. Morphology and marker expression analysis
   ➢ 5 biological replicates for each condition
   ➢ 2 technical replicates

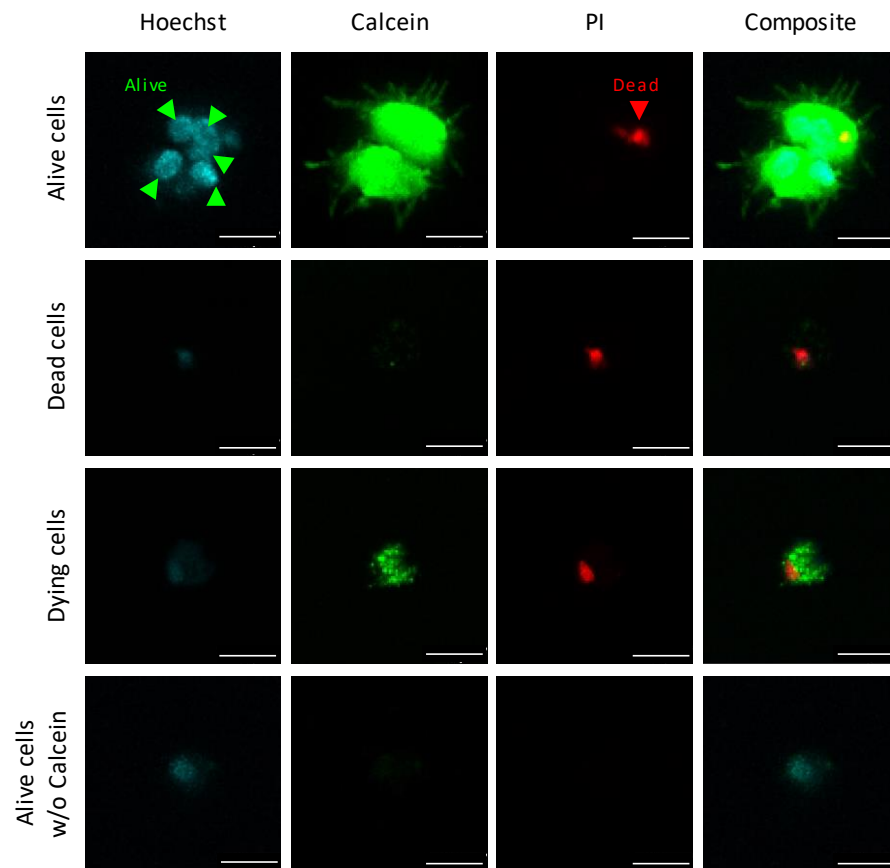# Result: Different CaCl$_2$ concentrations **do not impact** cell viability on FibrinVLVG hydrogels

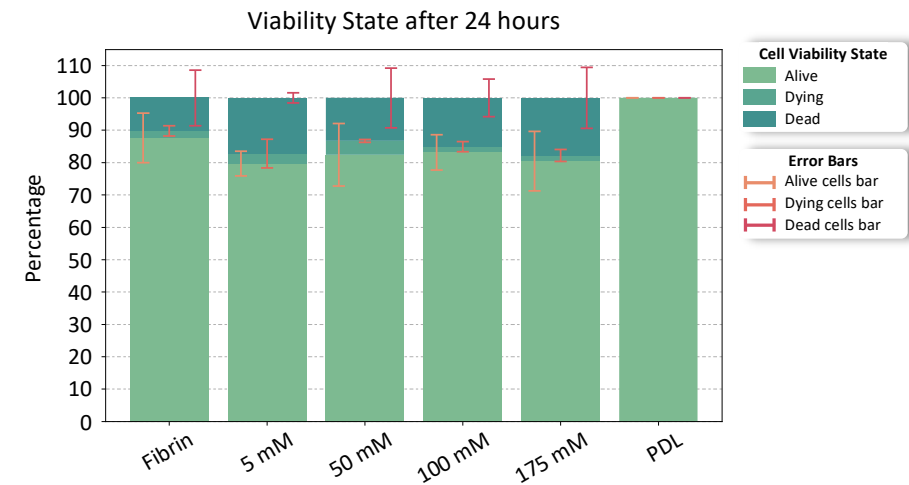**Figure 3.8.** Representative cells of each viability class.

Figure 3.9. Viability essay analysis on VLVG, FibrinVLVG hydrogels and monolayer cultures.

➢ **No correlation** between calcium levels and proportion of live or dead cells (Pearson and Spearman tests)

➢ Hydrogel cultures **might have increased cell stress** comparing to monolayer cultures

p5-7 WT | 1 technical replicate/biological replicate (N) | Hydrogels: N=3; PDL: N=4| Total of 1712 classified cells.

Result: Different CaCl$_2$ concentrations **impact** cell morphology and astrocyte marker expression
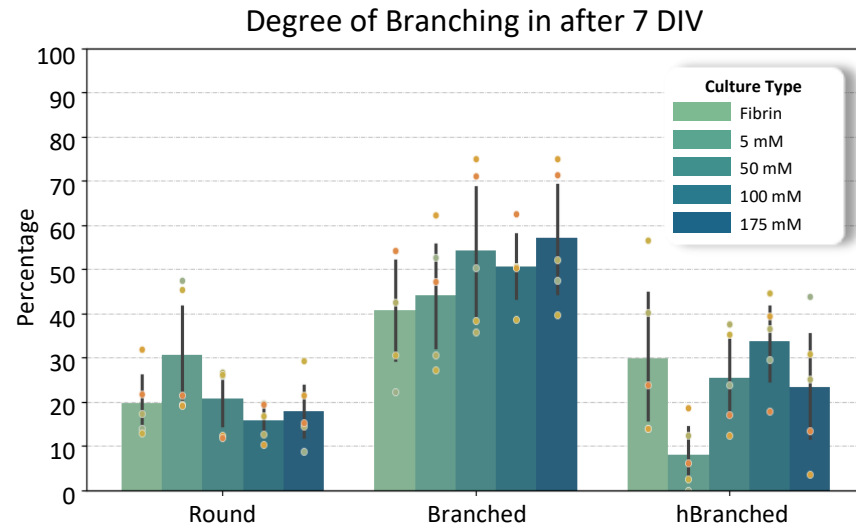
Figure 3.10. Effects of CaCl$_2$ concentration on cell morphology after 7 DIV.

Figure 3.11. Effects of CaCl$_2$ concentration on astrocyte marker expression after 7 DIV.

➤ **Higher Ca2+** concentrations show tendency to exhibit **more branched cells** (r = 0.32, p = 0.12)

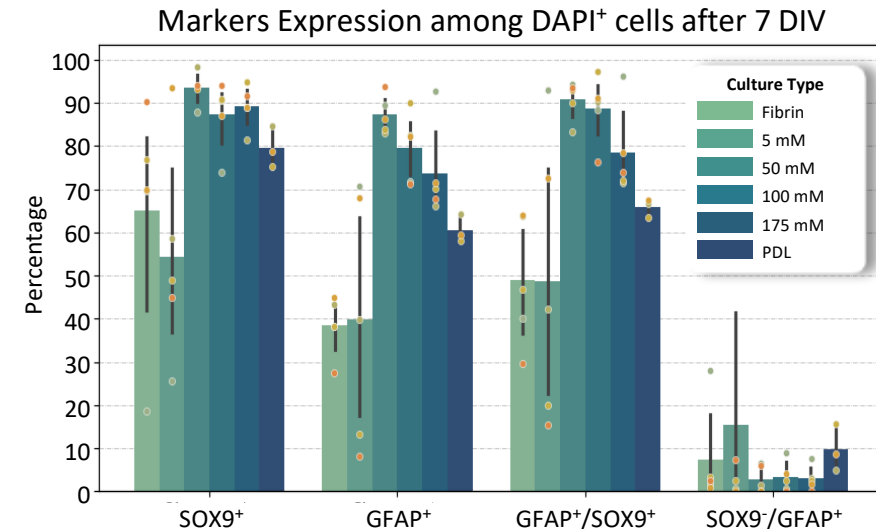➤ **Possibly Ca2+ increases stiffness** of the hydrogels allowing more branched structures

➤ Fibrin and 5mM show high variation and low reliability (excluded from evaluation)

➤ **Higher Ca2+** concentration used for gelation generally leads to **less GFAP+ expression** (r = -0.6, p = 0.02)

➤ Hydrogels show **higher GFAP+/SOX9+ reactive profiles** (*t*-test, p = 0.02)

04 Conclusion

Conclusions

1 **Experimental validation of hydrogel matrices**

- ❖ FibrinVLVG hydrogels (50 – 175 mM $CaCl_2$) stable for 7 DIV cultures
- ❖ Elevated $CaCl_2$ concentrations did not decrease cell viability
- ❖ $CaCl_2$ concentration **tendency to increase cell branching** (no significant effect)
- ❖ Higher $CaCl_2$ concentrations produced **less GFAP$^+$ reactive** profiles

2 **Computational solutions to nuclei segmentation and assisted cell classification**

- ❖ High performing nuclei segmentation model – error rate <5% on hydrogel images
- ❖ GUI for z-stack image annotation targeting cell nuclei

Limitations and Future Work

EXPERIMENTAL WORK

Limited understanding of hydrogel properties

- ❖ Interactions scaffold-substrate
- ❖ Hydrogel physical and chemical properties

Limited understanding of astrocyte cultures

- ❖ Phenotypic studies (e.g. RNA-seq, gene expression)
- ❖ Cell function (e.g. motility, calcium imaging)
- ❖ Increase biological replicates

COMPUTATIONAL WORK

Scarcity of annotated data and Limited generalizability

- ❖ Fine-tuning pretrained models with annotated data
- ❖ Increase dataset size and diversity

Limited GUI versatility

- ❖ Real time cell position prediction
- ❖ Configurable classification labels

Limited cell characterization

- ❖ Analysis of nuclei properties
- ❖ Automatic morphology classification

References

Bocchi, R., Thorwirth, M., Simon-Ebert, T., Koupourtidou, C., Clavreul, S., Kolf, K., ... & Fischer-Sternjak, J. (2025). Astrocyte heterogeneity reveals region-specific astrogenesis in the white matter. *Nature Neuroscience*, 1-13. https://doi.org/10.1038/s41593-025-01878-6

Pereira, A., Diwakar, J., Masserdotti, G., Beşkardeş, S., Simon, T., So, Y., ... & Götz, M. (2024). Direct neuronal reprogramming of mouse astrocytes is associated with multiscale epigenome remodeling and requires Yy1. *Nature Neuroscience*, *27*(7), 1260-1273.

Park, J. H., Jo, S. B., Lee, J. H., Lee, H. H., Knowles, J. C., & Kim, H. W. (2022). Materials and extracellular matrix rigidity highlighted in tissue damages and diseases: Implication for biomaterials design and therapeutic targets. *Bioactive materials*, *20*, 381–403. https://doi.org/10.1016/j.bioactmat.2022.06.003

Jurga, A. M., Paleczna, M., Kadluczka, J., & Kuter, K. Z. (2021). Beyond the GFAP-astrocyte protein markers in the brain. *Biomolecules*, *11*(9), 1361. https://doi.org/10.3390/biom11091361

Matias, I., Morgado, J., & Gomes, F. C. A. (2019). Astrocyte Heterogeneity: Impact to Brain Aging and Disease. *Frontiers in aging neuroscience*, *11*, 59. https://doi.org/10.3389/fnagi.2019.00059

Miller, S. J. (2018). Astrocyte heterogeneity in the adult central nervous system. *Frontiers in cellular neuroscience*, *12*, 401. https://doi.org/10.3389/fncel.2018.00401

Fernandes, M. B. S. (2025). *Characterization of Murine Astrocyte Cultures in 3D Hydrogel Matrices*. [Master's thesis, Instituto Superior Técnico, Universidade de Lisboa]

Thank you!

Maria Beatriz Sereno Fernandes

March 2025